ELSEVIER

Journal of Structural Geology 27 (2005) 731–743

JOURNAL OF STRUCTURAL GEOLOGY

www.elsevier.com/locate/jsg

Rotation of single rigid inclusions embedded in an anisotropic matrix: a theoretical study

Nibir Mandal, Santanu Misra, Susanta Kumar Samanta*

Department of Geological Sciences, Jadavpur University, Kolkata 700032, India

Received 23 March 2004; received in revised form 2 December 2004; accepted 20 December 2004

Abstract

This paper presents a theoretical analysis of instantaneous rotation of elliptical rigid inclusions hosted in a foliated matrix under bulk tensile stress. The foliated matrix is modelled with orthotropic elastic rheology, considering two factors as measures of anisotropy: $m = \mu^0/E_1^0$ and $n = E_2^0/E_1^0$, where μ^0 is the shear modulus parallel to the foliation plane and E_1^0 and E_2^0 are the Young moduli along and across the foliation, respectively. Normalized instantaneous inclusion rotation (ω) is plotted as a function of the bulk tension direction (α) with respect to the long axis of the inclusion, taking into account two parameters: (1) anisotropic factors m and n, and (2) the inclination of the foliation plane to the long axis of inclusion (θ). In the case of $\theta = 0°$, ω versus α variations are sinuous, showing maximum instantaneous rotation in positive and negative sense at $\alpha = 45$ and 135°, respectively, irrespective of m and n values. The magnitude of maximum ω increases with decrease in m, i.e. increasing degree of anisotropy in the matrix. On the other hand, decreasing the value of the anisotropic factor n results in decreasing instantaneous rotation. ω increases with the aspect ratio R of inclusion, assuming an asymptotic value when R is large. This asymptotic value is larger for lower values of m. In case of $\theta \neq 0°$, ω versus α variations are asymmetrical, showing maximum instantaneous rotation at varying inclusion orientation for different m. For given m and n, with increase in θ the sense of instantaneous rotation reverses at a critical value of θ.

Keywords: Anisotropy factors; Complex variables; Tensile stress; Inclusion rotation

1. Introduction

One of the aspects in the structural study of inclusion-matrix rock systems is understanding the rotational motion of rigid inclusions and how that motion perturbs the flow of matrix around them. Based on Jeffery's (1922) theory, Gay (1968) presented an analysis on the rotation of elliptical inclusions as a function of their shape and orientation, considering bulk deformation in pure shear. Ghosh and Ramberg (1976) used the same theory in studying the rotation behaviour for general type bulk deformations involving both pure shear and simple shear. In their derivation they consider the equation of instantaneous rotation for pure shear given by Muskhelishvili (1953). Later studies (Freeman, 1985; Passchier, 1987; Jezek et al., 1996; Mandal et al., 2001) have employed the general expressions of Jeffery it is possible to analyse the rotation of inclusions either in two- or three dimensions for any type of homogenous bulk flow.

Analyses based on either Jeffery's or Muskhelishvili's theory are applicable to inclusions floating in a mechanically isotropic matrix. In many geological situations, the matrix show structural fabrics, e.g. foliations, lineations, which are likely to induce mechanical anisotropy in the matrix (Cobbold, 1976; Weijermars, 1992; Mandal et al., 2000; Treagus, 2003; Fletcher, 2004). In spite of significant development on the study of inclusion-matrix systems, there is some lacuna in our understanding of how such anisotropy in the matrix can influence the rotation behaviour of rigid inclusions. In this paper we make an attempt, employing the theory of elasticity, to understand the rotation behaviour of single rigid inclusions embedded in an orthotropically anisotropic matrix (Ramsay and Lisle, 2000). The results obtained from the analysis are compared with those for an isotropic matrix (Muskhelishvili, 1953) in order to show variations of inclusion rotation as a function of the degree of mechanical anisotropy in the matrix.

* Corresponding author. Tel.: +91 33 414 6214; fax: +91 33 856 0008.
E-mail address: susanta_ju@hotmail.com (S.K. Samanta).

0191-8141/$ - see front matter © 2005 Elsevier Ltd. All rights reserved.
doi:10.1016/j.jsg.2004.12.005

2. Theoretical considerations

2.1. Measures of mechanical anisotropy

The elastic parameters of an orthotropic medium can be described in two dimensions as:

$$\begin{bmatrix} a_{11}^0 & a_{12}^0 & 0 \\ a_{12}^0 & a_{22}^0 & 0 \\ 0 & 0 & a_{66}^0 \end{bmatrix} \quad (1)$$

where $a_{11}^0 = 1/E_1^0$, $a_{12}^0 = \nu_{12}/E_1^0$, $a_{22}^0 = 1/E_2^0$ and $a_{66}^0 = 1/\mu^0$. E_1^0 and E_2^0 are the Young's moduli along and across the foliation, respectively (Fig. 1a and b). ν_{12} is the Poisson's ratio. μ^0 is the shear modulus parallel to the foliation (Fig. 1c). In our analysis we consider two dimensionless anisotropic factors (cf. Ramsay and Lisle, 2000):

$$m = \frac{\mu^0}{E_1^0} \quad \text{and} \quad n = \frac{E_2^0}{E_1^0}. \quad (2)$$

2.2. General mathematical approach

Consider an elliptic cylindrical rigid inclusion within an infinite orthotropic matrix (Ramsay and Lisle, 2000). The cylindrical axis of the inclusion is assumed to lie on the foliation. Our analysis will be in two dimensions, considering a section at a right angle to the inclusion axis, i.e. parallel to the elliptic section of the inclusion. The semi-axes of the inclusion on this section are a and b. A Cartesian frame xy is chosen with the x axis along the a axis (Fig. 2). The foliation is at an angle of θ to the x-axis. The bulk system is subjected to a far-field tension σ^∞ at angle α to the a axis of inclusion. Following the conventional approach (e.g. Muskhelishvili, 1953; Savin, 1961), we consider the bulk state of stress as tensile. In some geological situations, e.g. shear zones, rocks can deform under shear stresses. In that case, analysis has to be made considering a shear stress (τ^∞) as the far field stress. Different constants defining the bulk state of stress (Eqs. (A21a)–(A21c)) will thus change accordingly (eq. 1.98 of Savin, 1961).

Considering a plane strain condition, the general relations between stress and strain components can be written as:

$$\begin{aligned} \varepsilon_x &= a_{11}\sigma_{xx} + a_{12}\sigma_{yy} + a_{16}\sigma_{xy}, \\ \varepsilon_y &= a_{12}\sigma_{xx} + a_{22}\sigma_{yy} + a_{26}\sigma_{xy}, \\ 0 &= a_{16}\sigma_{xx} + a_{26}\sigma_{yy} + a_{66}\sigma_{xy} \end{aligned} \quad (3)$$

After transformation of the matrix (Eq. (1)) (Lekhnitskii, 1981; Chandrupatla and Belegundu, 2001), the elastic parameters in Eq. (3) can be written in the form of following equations:

$$\begin{aligned} a_{11} &= a_{11}^0 \cos^4\theta + (2a_{12}^0 + a_{66}^0)\sin^2\theta\cos^2\theta + a_{22}^0 \sin^4\theta, \\ a_{22} &= a_{11}^0 \sin^4\theta + (2a_{12}^0 + a_{66}^0)\sin^2\theta\cos^2\theta + a_{22}^0 \cos^4\theta, \\ a_{12} &= (a_{11}^0 + a_{22}^0 - 2a_{12}^0 - a_{66}^0)\sin^2\theta\cos^2\theta + a_{12}^0 \end{aligned} \quad (4)$$

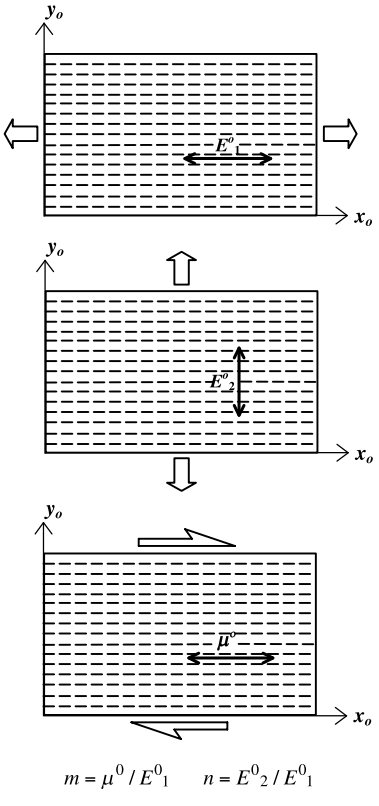

Fig. 1. Definition of anisotropic factors m and n. E_1^0 and E_2^0 are Young's moduli of orthotropic matrix under tensile stresses (block arrows) acting parallel and perpendicular to the anisotropic plane in (a) and (b), respectively. μ^0 is the shear modulus of the matrix under shear stress (block arrows) acting parallel to the anisotropic plane in (c).

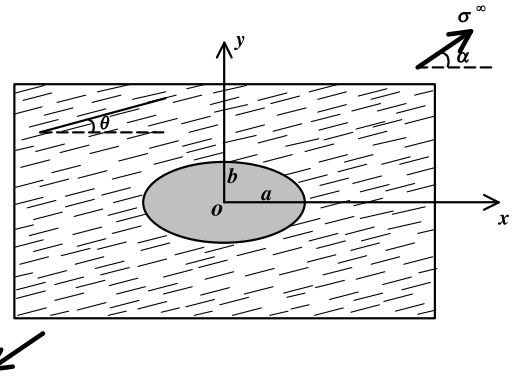

Fig. 2. A Cartesian coordinate frame oxy defined with respect to elliptical inclusion. a and b are the semi-axes of inclusion. σ is the angle of far-field tension σ^∞ to the x axis, and θ is the inclination of foliation (solid line) to the x axis.

$$a_{66} = 4(a_{11}^0 + a_{22}^0 - 2a_{12}^0 - a_{66}^0)\sin^2\theta\cos^2\theta + a_{66}^0,$$

$$a_{16} = [2a_{22}^0\sin^2\theta - 2a_{11}^0\cos^2\theta + (2a_{12}^0 + a_{66}^0) \times(\cos^2\theta - \sin^2\theta)]\sin\theta\cos\theta,$$

$$a_{26} = [2a_{22}^0\cos^2\theta - 2a_{11}^0\sin^2\theta - (2a_{12}^0 + a_{66}^0) \times(\cos^2\theta - \sin^2\theta)]\sin\theta\cos\theta$$

In the plane theory of elasticity the stress components can be expressed in terms of the Airy's stress function U, satisfying the following equation (Lekhnitskii, 1981):

$$a_{22}\frac{\partial^4 U}{\partial x^4} - 2a_{26}\frac{\partial^4 U}{\partial x^3\,\partial y} + (2a_{12} + a_{66})\frac{\partial^4 U}{\partial x^2\,\partial y^2} - 2a_{16}\frac{\partial^4 U}{\partial x\,\partial y^3} + a_{11}\frac{\partial^4 U}{\partial y^4} = 0 \quad (5)$$

The general solution of U (Eq. (5)) can be obtained using the roots of the following characteristic equation:

$$a_{11}s^4 - 2a_{16}s^3 + (2a_{12} + a_{66})s^2 - 2a_{66}s + a_{22} = 0 \quad (6)$$

The above equation is quartic, which will have four roots, for example, s_1, s_2, s_3 and s_4. It has been shown that all the roots will be necessarily complex (eq. 20.22, Lekhnitskii, 1981), which can be expressed as:

$$s_1 = \alpha_1 + \mathrm{i}\beta_1, \quad s_2 = \alpha_2 + \mathrm{i}\beta_2, \quad s_3 = \alpha_1 - \mathrm{i}\beta_1, \quad s_4 = \alpha_2 - \mathrm{i}\beta_2 \quad (7)$$

α_1, β_1, α_2 and β_2 are real constants, which depend on the elastic parameter a_{ij}. The derivations of these constants are given in Appendix A.1. Using Eq. (A9), their expressions follow:

$$\alpha_1 = -\frac{G}{2A}, \quad \alpha_2 = -\frac{g}{2A}, \quad \beta_1 = \frac{\sqrt{4AH - G^2}}{2A}, \quad \beta_2 = \frac{\sqrt{4Ah - g^2}}{2A} \quad (8)$$

The expressions of different parameters in Eq. (8) are cited in Appendix A.

2.3. Governing equation for inclusion rotation

Savin (1961) has developed a fundamental equation governing the instantaneous rotation of a rigid inclusion hosted in an orthotropic matrix under a uniaxial tension. The equation is obtained in a complex form (Eq. (A10)), which is difficult to use for any direct analysis. We have done considerable algebraic work with this equation (see Appendix A), and obtained the instantaneous rotation rate in the following form (Eq. (A24)):

$$\Omega = \frac{(F_1R_1 - \alpha_1E_1) - (H_1R_2 - \alpha_2G_1)}{(D_1R_2 - \alpha_2C_1) - (B_1R_1 - \alpha_1A_1)} \quad (9)$$

where $R_1 = R + \beta_1$, $R_2 = R + \beta_2$. R is the aspect ratio (a/b) of elliptical inclusion, α_1, α_2, β_1, β_2 are the roots of Eq. (6), the expressions of which are given in Eq. (8). A_1, B_1, C_1, D_1, E_1 and F_1 are different constants and their values depend on the elastic parameters (a_{ij}) and inclusion orientation α. The algebraic expressions for these constants are given in Appendix A (Eqs. (A17)–(A23)). It may be noted that, to find the instantaneous rotation in Eq. (9) we first need to find the roots in Eq. (8), for which all the preceding equations are required. Again, the determination of constants in Eq. (9) involves a set of equations derived in Appendix A. We developed a program in Basic with the mathematical equations, and the results obtained from the computations are presented in the following section.

3. Analysis of inclusion rotation

3.1. Case 1: inclusion oriented along fabric ($\theta = 0°$)

We first consider cases where the a axis of inclusion is parallel to the foliation (i.e. $\theta = 0°$, Fig. 2). The system is subject to far-field tensile stress σ^∞ at varying orientation α. In describing the instantaneous rotation of inclusion, Ω is normalized to $a_{11}^0\sigma^\infty$ and will be denoted as ω. It is evident that the instantaneous rotation ω will vary with α. In order to show the effect of mechanical anisotropy we determined ω versus α variations, and compared them with that obtained from the equation of Muskhelishvili (1953) for an isotropic matrix:

$$\Omega = \frac{\sigma^\infty}{2\mu}\frac{R^2 - 1}{R^2 + 1}\sin 2\alpha \quad (10)$$

where μ is the shear modulus, which in the present nomenclature is $1/a_{66}$. It may be noted that for isotropic materials the relation between the shear and Young's moduli is

$$\frac{\mu}{E} = \frac{1}{2(1 + \nu)}. \quad (11)$$

The ratio will tend toward 0.33 when the matrix is mechanically isotropic and incompressible ($\nu = 0.5$). It therefore follows that the matrix is anisotropic if the factor m is less than 0.33.

Using Eq. (9) we computed ω–α variations for different values of m and n factors (Figs. 3 and 4). The plots show that the normalized instantaneous rotation ω will be a maximum when the bulk tension direction is at an angle of 45 and 135° to the long axis of inclusion, irrespective of the degree of mechanical anisotropy, as in the case for isotropic matrix (Eq. (10)). The inclusion remains stable when the bulk tension direction is either parallel or perpendicular to the long axis of the inclusion.

When m is 0.33, the magnitude of instantaneous inclusion rotation is close to that obtained for isotropic

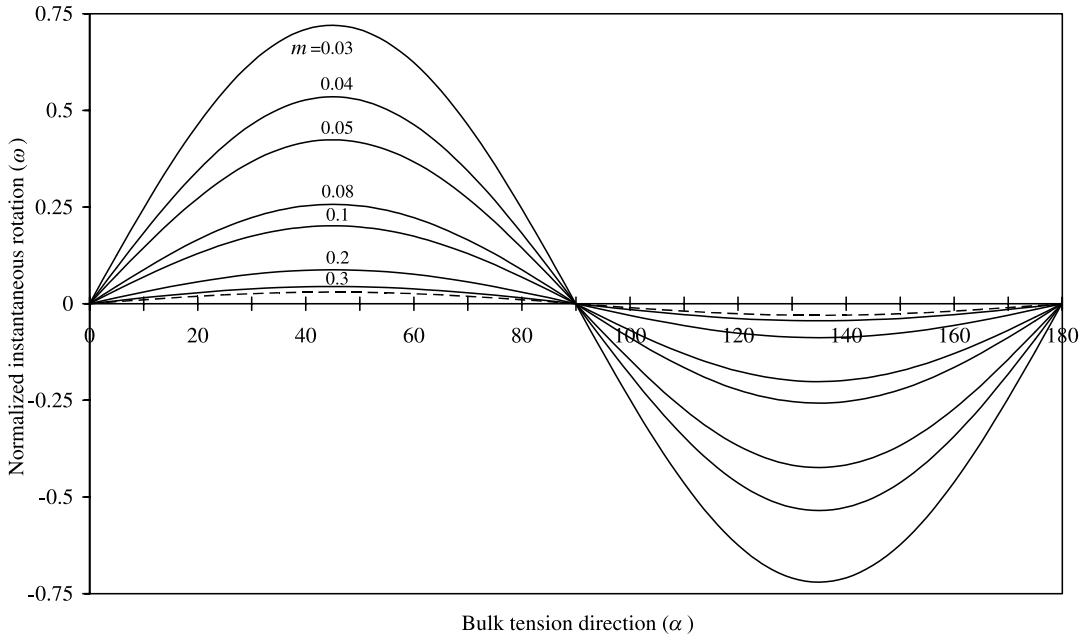

Fig. 3. Calculated plots of instantaneous inclusion rotation (ω), normalized to $a_{11}\sigma^{\infty}$, as a function of bulk tension direction for different m values. Dashed line represents the plot for isotropic matrix obtained from the equation of Muskhelishvili (1953). $R=3$, $n=1$, $\theta=0°$.

matrix (Eq. (10)). For any inclusion orientation, the instantaneous rotation shows a departure from the isotropic value when m is less than 0.33 (Fig. 3). Decreasing m, i.e. enhancing the degree of mechanical anisotropy, promotes the instantaneous rotation in positive and negative directions for $\alpha<90$ and $>90°$, respectively. For example, the instantaneous rotation is a maximum at $\alpha=45°$, which is less than 0.1 when $m=0.3$. The maximum value exceeds 0.25 when m becomes less than 0.1. The theoretical results suggest that the instantaneous rotation of rigid inclusions during deformation of a rock can vary to a large extent due to the foliated nature of the rock. For example, an obliquely oriented inclusion within a massive bed rotates at a certain rate under a bedding-parallel tensile stress. Inclusions of the same orientation, but hosted in a foliated bed will rotate at different rates, and the difference will be larger for higher degrees of mechanical anisotropy imparted by the foliation.

The effect of anisotropic factor n, the ratio of Young's

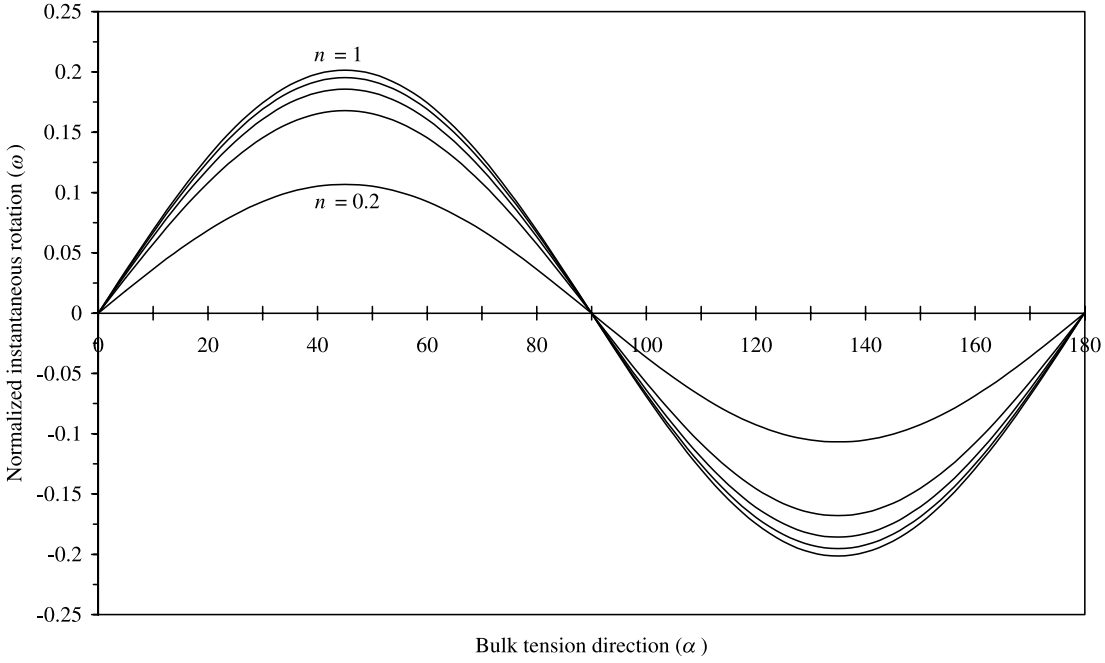

Fig. 4. Variation of ω with α for different n values. $R=3$, $m=0.1$, $\theta=0°$.

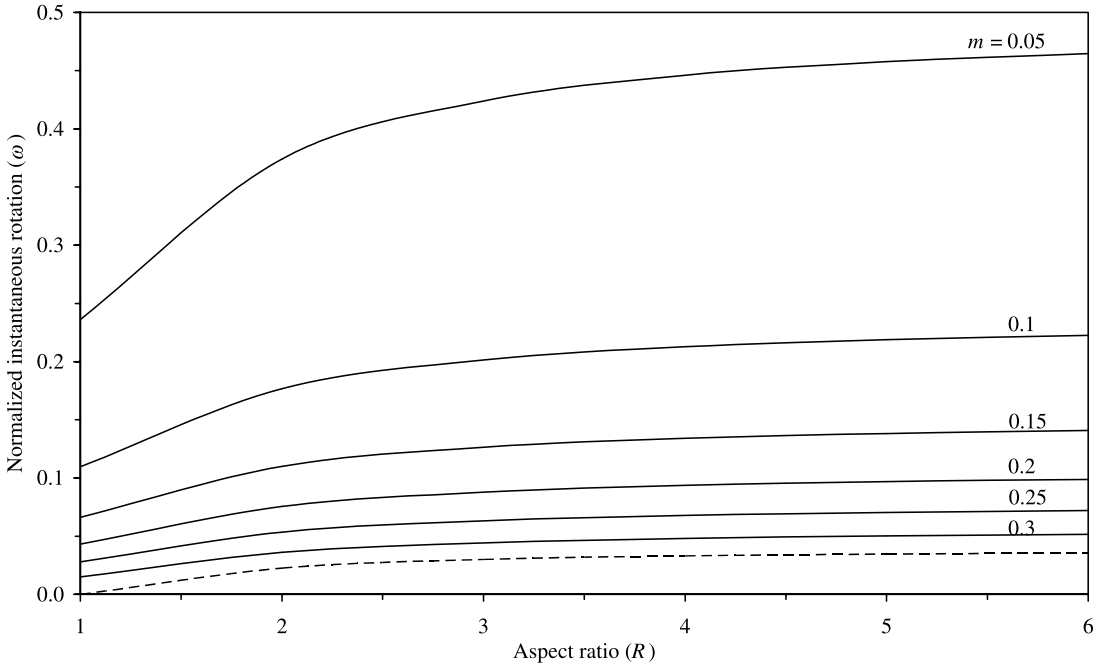

Fig. 5. Calculated plots of ω as a function of inclusion aspect ratio R for different m values. $n=1$. Dashed line represents the variation for isotropic matrix. $\theta=0°$, $\alpha=45°$.

modulus across and along the foliation, acts in the opposite sense to m. For a given m, say 0.1, decreasing n lowers the instantaneous rotation of inclusion (Fig. 4). The maximum of instantaneous rotation at $\alpha=45°$ is about 0.2 when $n=1$. The value decreases down to 0.1 when $n=0.2$. However, the effect of this factor on the inclusion rotation is not as strong as in the previous one. Increasing the mechanical anisotropic factor n from 0.2 to 1 lowers the instantaneous rotation to half. In contrast, decreasing the anisotropic factor m from 0.3 to 0.05 enhances inclusion rotation by more than 10 times. The numerical calculations suggest that changes in the value of anisotropic factor m exert more effect on the instantaneous rotation of inclusion, relative to that of anisotropic factor n. m is a ratio of shear and Young's moduli with respect to the foliation. It seems that decreasing m would increase shear strain component along the foliation, which possibly results in higher instantaneous rotation of inclusion oriented at an angle to the bulk tension direction. On the other hand, the anisotropic factor n has less effect in promoting shearing strain along the foliation, and thereby brings about comparatively small changes in the instantaneous rotation.

It is evident from Eq. (10) that the instantaneous rotation is also a function of inclusion aspect ratio R, and that it tends to assume an asymptotic value as R becomes very large (Fig. 5). By varying the anisotropic factor m, we investigated how much the ω versus R relation can show departures owing to the foliated nature of the matrix. Plots of ω–R for $\alpha=45°$ and $\theta=0°$ reveal that an inclusion with $R=1$, i.e. circular shape, does not rotate when the matrix is isotropic. In contrast, there is a finite instantaneous rotation when the matrix is anisotropic. For a given value of m, the rotation initially increases with increase in R, but becomes progressively insensitive to R, and assumes a stable value, as in the case of isotropic matrix. Instantaneous rotation of an inclusion for varying R, overall, is larger for higher degrees of anisotropy in the matrix. Secondly, when R is low to moderate, the sensitivity of ω to R increases with increase in anisotropy, as reflected by the increasing gradient in ω versus R curves.

3.2. Case 2: inclusion oriented oblique to fabric ($\theta>0°$)

We analysed the effects of foliation orientation on the instantaneous rotation of inclusions (Fig. 6). The analyses were performed considering ω–α variations for different θ, where the anisotropy factors m and n were kept constant. We first present results obtained for $m=0.05$ and $n=1$. The plots show that the rotation behaviour can significantly change depending on the foliation orientation under the same stress condition. When $\theta=0°$, ω varies sinuously with α, and the variation is symmetrical, showing a maximum and a minimum at $\alpha=45$ and 135°, and stable positions at $\alpha=0$ and 90°. The nature of variation changes with increase in θ. For $\theta=20°$, the curve is asymmetrical, showing stable positions at $\alpha=72$ and 128°. The curve indicates that inclusions with their long axis parallel or perpendicular to the bulk tension direction can rotate, which is not possible if

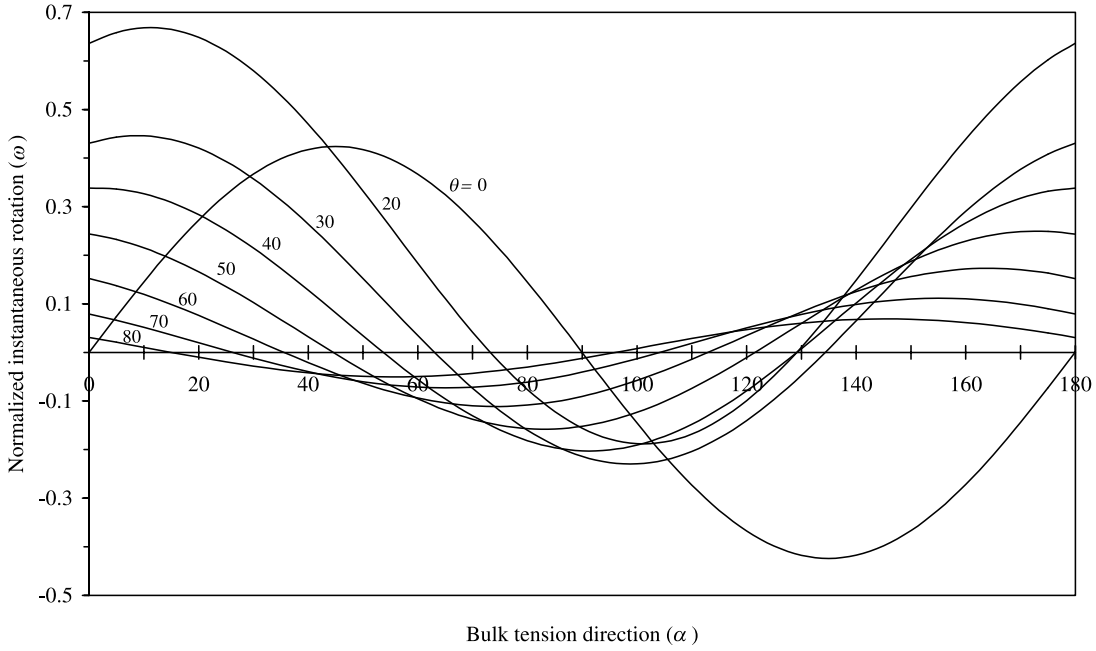

Fig. 6. Influence of foliation orientation (θ) on ω–α variations. $R=3$, $m=0.05$, $n=1$.

the matrix is mechanically isotropic. Secondly, an inclusion oriented at an angle of 12° to the tension direction will experience rotation with maximum magnitude, whereas the rotation in the negative direction will be maximum when $\alpha=100°$. However, the latter will be much less than the maximum positive rotation. With progressive increase in θ, the amplitudes of the curves and their positions vary, implying changes in the rotation behaviour of rigid inclusion. The sense of inclusion rotation varies with α, defining fields of positive and negative rotation, which are different for different foliation orientations (Fig. 7).

The effects of foliation orientation on the instantaneous rotation of inclusion can be summarized as follows. (1) Inclusions oriented parallel or perpendicular to the bulk tension direction may not remain stable, as they would in an isotropic matrix. (2) Inclusions oriented parallel to the bulk tension direction will rotate in the positive direction if the foliation is oblique and the magnitude of rotation will increase to a maximum and then drop with further increase in θ. (3) Under the same stress conditions, inclusions of the same orientation may show contrasting sense of rotation for different orientations of matrix foliation. For example, inclusions oriented at an angle less than 90° will always rotate in the positive sense when the foliation is parallel to the long axis of inclusion. On the other hand, inclusions of the same orientation can rotate in the negative sense if the foliation is at a high angle; say 70°, to the long axis of inclusion (Fig. 7). (4) Instantaneous rotation of inclusions decreases as the angle between the foliation and the long axis of inclusion increases. (5) The directions of bulk tension with respect to the inclusion axis define the fields of negative and positive inclusion rotation, which vary with the foliation orientation (Fig. 7). (6) Inclusion orientation giving maximum instantaneous rotation varies with foliation orientation. The orientation is 45° when foliation is parallel to the inclusion axis. The angle decreases with increases in the foliation inclination, becomes zero when the foliation inclination is about 40°, and finally negative when the inclination is larger than 45°.

We performed a set of numerical runs considering $n<1$ and analysed how the anisotropy factor n can influence the rotation behaviour of inclusion under varying foliation orientations. The results obtained for $n=0.8$ are presented here (Fig. 8). The plots show that ω versus α variations for different foliation orientations are different when the anisotropy factor n is introduced. The positions of the ω–α curves change as n becomes less than 1. For $\theta=0°$, the curve is symmetrical, indicating equal fields of positive and negative rotation in the ranges of $\alpha<90$ and $>90°$, respectively. When θ is increased to 10°, the curve becomes asymmetrical, showing positive rotation in a narrow range of α (22–78°), and negative rotation in a wider range. The maximum value of instantaneous rotation in the positive sense is much less compared with that of negative rotation. ω is a maximum at $\alpha\approx50°$, in contrast to 45° when $\theta=0°$. With further increases in θ, ω–α curves change drastically. They show negative rotation over a narrow range of α (80–100°), which increases slightly with increase in θ. The maximum of this negative rotation occurs when α is close to 90°, whereas that of positive rotation occurs when α is nearly 0. The magnitude of negative rotation, overall, is much less than that of positive rotation. The orientations of inclusions showing maximum rotation in the positive and negative sense do not vary

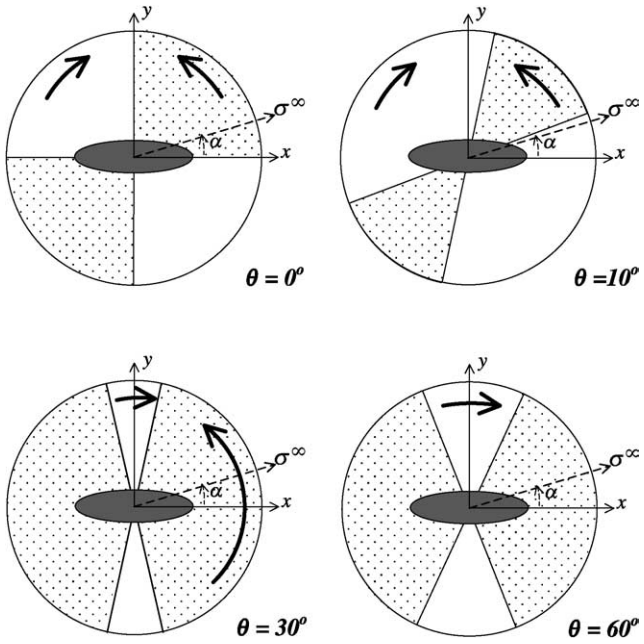

Fig. 7. Fields for inclusion rotation in positive (stippled) and negative sense (blank) for different foliation orientation θ. Dashed arrow indicates the direction of far-field tension σ^{∞}. Note that the lines separating the fields are the direction of tension in which the inclusions remain stable.

significantly with θ as well as the value of the anisotropic factor n. The theoretical results imply that rigid inclusions in foliated rocks will have a tendency to rotate largely in the positive sense when the foliation orientation exceeds a critical value (Fig. 9). It is found that there is a jump in the position of ω–α curves when θ exceeds 10°. We studied the critical value of θ where this drastic change occurs, considering the nature of ω–θ variation at $\alpha = 0°$. The plot shows that ω decreases monotonically with θ, but jumps to a large positive value, and then sharply drops to a low value. The break point in ω versus θ curves separates the fields of negative and positive rotation. A rigid inclusion oriented parallel to the bulk tension direction will rotate in the negative direction when the foliation is inclined at an

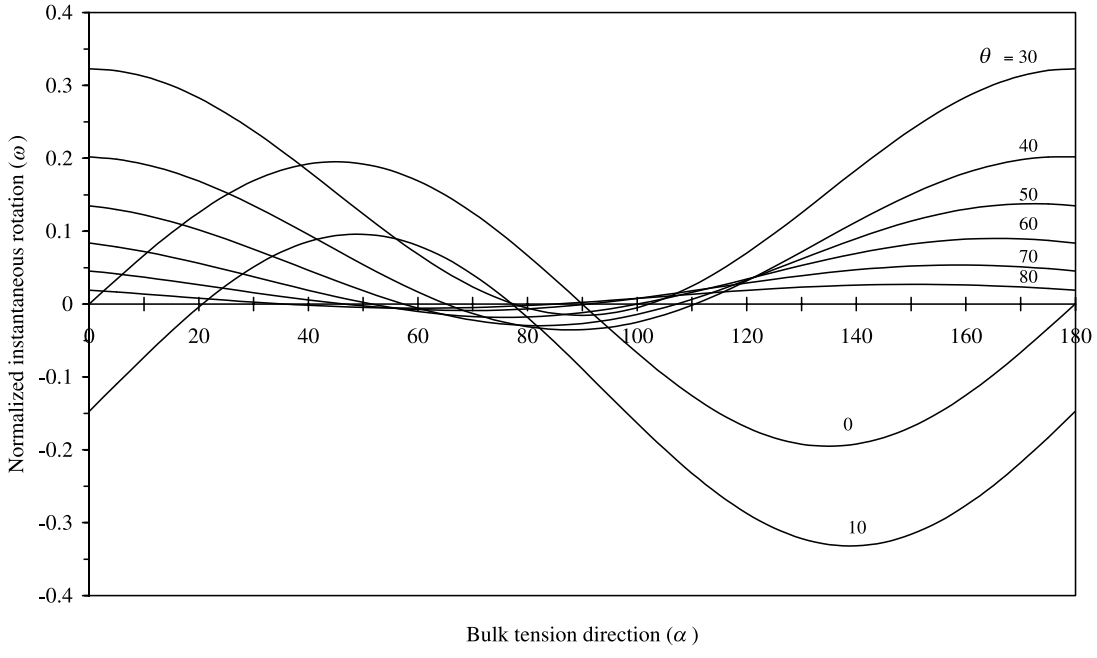

Fig. 8. A general case of ω–α plots for different foliation orientation θ. See text for detailed description. $n = 0.8$.

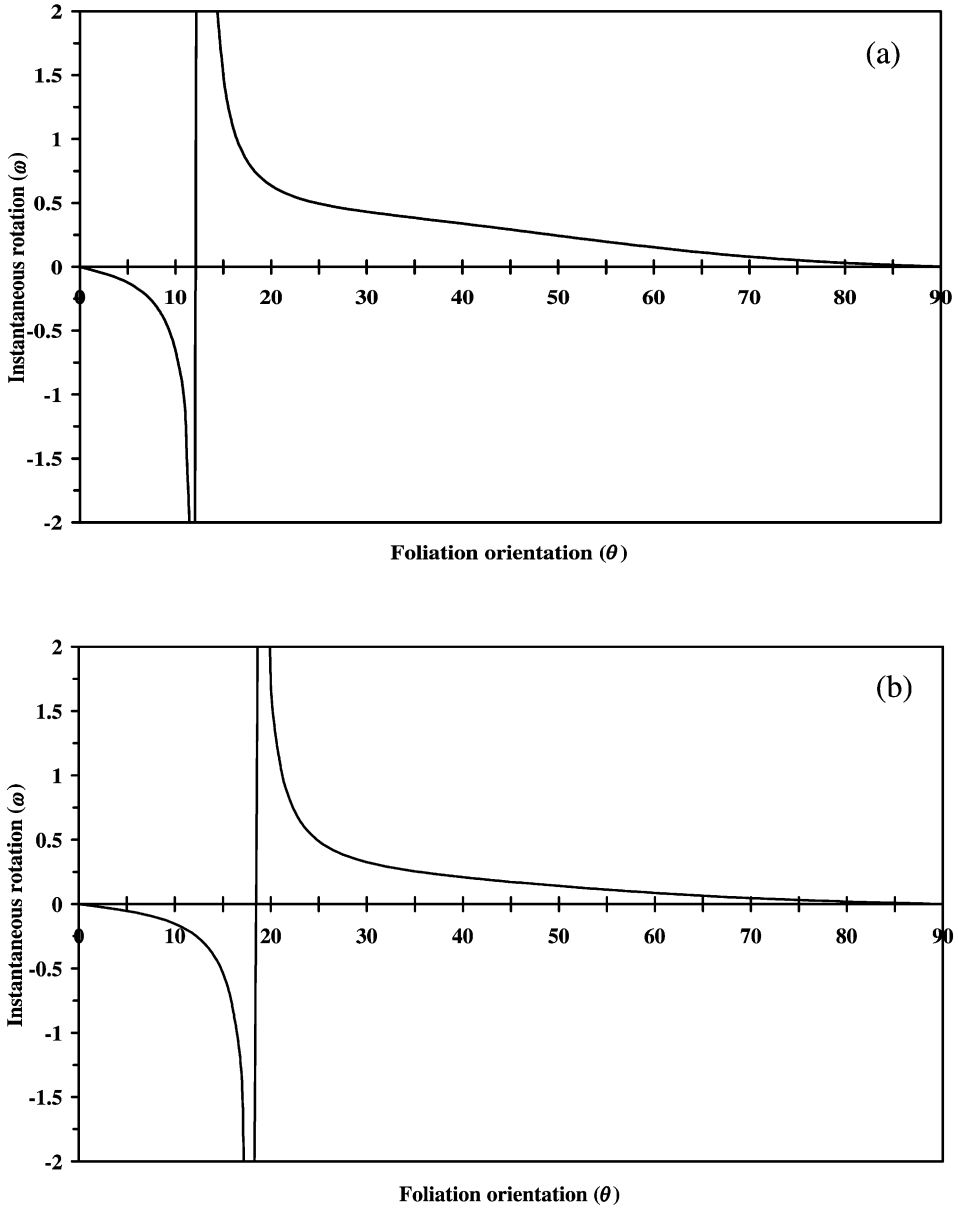

Fig. 9. Plots showing variation of ω with foliation orientation θ under a given orientation of far-field tension ($\alpha=0$). (a) $m=0.05$, $n=1$ and (b) $m=0.01$, $n=1$. Note that the sharp breaks in the curves indicate reversal in the sense of inclusion rotation.

angle less than about 18° to the long axis of inclusion. Under the same stress condition, the inclusion will rotate in the positive direction if the foliation is oriented at angles larger than 12°. This critical θ increases slightly with decrease in n values.

4. Discussion

The analytical results presented in the preceding sections suggest that mechanical anisotropy in the matrix can lead to significant departures in rigid rotation of inclusions obtained from the theory based on isotropic matrix (Muskhelishvili, 1953). Under a given bulk stress, the rotation of inclusions with the long axis oriented parallel to the plane of anisotropy increases with decreasing value of the factor m, ratio of shear and Young's moduli. Normalized instantaneous rotation obtained for $m=0.33$, i.e. isotropic matrix is 0.05, which increases to 0.5 when the matrix is anisotropic with $m=0.04$. The results imply that the presence of foliation in the matrix is likely to enhance inclusion rotation in inclusion-matrix systems subjected to bulk tension at an angle to the long axis of inclusion. On the other hand, the anisotropic factor n, ratio of Young's moduli across and along the foliation, exerts a

contrasting effect on inclusion rotation. For a given m, the instantaneous rotation decreases with decreasing n. However, the effect of m factor appears to be much more dominant compared with that of the n factor.

In the kinematic analyses of inclusion-associated structures, such as foliation drag, porphyroblast trails, in schistose or laminated rocks, inclusion rotation is generally deduced from the theory based on isotropic matrix. For example, normal and reverse drag of foliation in the neighbourhood of a rigid inclusion have been explained considering the relative rotation of inclusion to the foliation, where the foliation is assumed to rotate like passive markers. However, the foliation that defines the structures itself imparts mechanical anisotropy in the rock, as reflected in recent studies (Mandal et al., 2000; Treagus, 2003; Fletcher, 2004). Our theoretical study indicates that foliations in the matrix can modify the instantaneous rotation behaviour of inclusion to a large extent and, depending on the degree of mechanical anisotropy in the matrix, the rotation of inclusion relative to the foliation can show contrasting senses. Analysis of rotational structures in foliated rocks and their use as kinematic indicators should thus be made with care. A large population of inclusions should be studied before conclusions are reached about the overall sense of rotation.

Following Ramsay and Lisle (2000), we have considered two factors m and n as measures of anisotropy. The factor m is the ratio of shear and Young's moduli, which is comparable with δ-factor used in several recent studies (Honda, 1986; Weijermars, 1992; Mandal et al., 2000; Treagus, 2003). δ is the ratio of shear and normal viscosity, which represent the flow resistance of the viscous medium to shear and normal stresses to the foliation, respectively. There is a slight difference between the two parameters. The value of δ factor is one, whereas that of m factor will be a function of ν, if the rock is isotropic. Assuming the isotropic material is incompressible, m will be 0.33, as $\nu = 0.5$. However, both the factors imply similar physical meaning. Lower values in both m and δ suggest higher degrees of anisotropy imparted by planes of weakness, such as schistosity, laminations, where the resistance to deformation under schistosity-parallel shear stress is much less than that under schistosity along tensile stress. The anisotropic factor n is equivalent to the σ-factor of Mandal et al. (2000), which is a measure of anisotropy in viscosity across and along a linear fabric. Both the parameters are a measure of anisotropy in resistance to flow parallel and perpendicular to a linear fabric. Our analysis with the n factor is also relevant to the study of rotation of rigid inclusions in lineated rocks. The theoretical results indicate that the instantaneous rotation can show large departures from that predicted for isotropic matrix if the lineation imparts strong anisotropy in the matrix, and is at an angle to the bulk tension direction.

The theoretical analysis presented in this paper is in two dimensions, considering plane strain condition and the rotation axis of inclusion along the direction of no-strain. The rotation behaviour of rigid inclusions in three-dimensional space is complex even when the matrix is isotropic (Freeman, 1985; Passchier, 1987). In the case of an anisotropic matrix, additional complexities are likely to occur as the expression of anisotropy in 3D will be larger than that given in Eq. (1) (Lekhnitskii, 1981; Ramsay and Lisle, 2000). Our analysis assumes that the rotation axis of inclusion lies on the plane of anisotropy. In natural situations this may occur at an angle, and the rotation of inclusion will depend on this angle. Evidently, our analysis is based on ideal boundary conditions, but provides a first hand idea on how the presence of foliation or lineation can affect the instantaneous rotation of a rigid inclusion.

There are some limitations in the present theoretical approach, which are discussed along the following points. (1) The theoretical analysis deals with instantaneous rotation of elongate rigid inclusions. In the analysis the mathematical equation describing the rotation remains valid till the foliation around the inclusion is planar. With progressive deformation the foliation is likely to be distorted to curved geometry, as the inclusion undergoes large rotation, exerting a drag effect on the surrounding matrix. It is not possible to utilize the theory to determine the finite rotations of inclusion employing any iterative solution method. The state of stress around the inclusion would become complex, as the foliation defining the anisotropy in the matrix assumes strongly curved geometry. Evidently, it is a limitation of our analysis that the present theoretical approach is applicable for small amounts of deformation. However, the results obtained from the analysis clearly reveal that the rotational behaviour of rigid inclusions in an anisotropic system would differ from that in an isotropic one. (2) Rigid inclusions are often associated with foliation drags resembling fold structures. Several workers have modelled the development of these structures employing hydrodynamic theories (Masuda and Ando, 1988; Bjørnerud, 1989; Jezek et al., 1999; Mandal et al., 2001). With the help of an iterative method it is possible to simulate complex fold structures on a foliation of passive nature. In our analysis the foliation is assumed to be mechanically anisotropic, and one can determine the curvilinear geometry of the foliation employing the displacement functions given by Savin (1961). However, it is not possible to simulate complex fold structures in the vicinity of rigid inclusions that are produced at large finite strains, as the functions will no longer remain valid when the foliation surfaces become curved following large rotations in rigid inclusion. (3) We present this theoretical analysis considering that the inclusion is coherent to the matrix. Incoherence may develop at the inclusion-matrix interfaces. The degree of incoherence would be an additional factor in determining the instantaneous rotation of rigid inclusion in anisotropic matrix (cf. Bjørnerud and Zhang, 1995).

5. Conclusions

Based on the theoretical analysis we conclude our paper with the following points:

(1) Shape fabrics, e.g. foliation, lineation, induce mechanical anisotropy in the matrix, which can in turn influence the instantaneous rotation of rigid inclusions under bulk tensile stresses.
(2) For both an isotropic and an anisotropic matrix, the instantaneous rotation of an inclusion varies as a sine function of inclusion orientation with respect to the bulk tension direction, showing maximum rotation in the positive and negative sense at 45 and 135°, respectively.
(3) In the case of an anisotropic matrix, the magnitude of maximum rotation depends on two anisotropic factors: m and n, where m is the ratio of shear modulus and Young's modulus along the foliation and n is the ratio of Young's moduli across and along the foliation. Decreasing m, i.e. increasing degree of anisotropy enhances inclusion rotation. On the other hand, the instantaneous rotation is comparatively less sensitive to the anisotropic factor n, but shows a conspicuous decreasing tendency with decreasing value of n.
(4) The orientation of the foliation with respect to the inclusion is another crucial parameter in controlling the rotation behaviour of rigid inclusions. Instantaneous inclusion rotation shows asymmetrical variation with the direction of bulk tension when the foliation is at an angle to the long axis of inclusion. For a given m, the sense rotation reverses at a critical foliation orientation.

Acknowledgements

We wish to thank Professors M. Bjørnerud and J. Hippertt for their valuable comments on the manuscript. The Department of Science and Technology, India has provided financial support in carrying out this work. Jadavpur University is gratefully acknowledged for extending a research fellowship to SM.

Appendix A

A.1. Solution of equation

In this section we present the method for obtaining the solution of quartic equations (Eq. (6)), which is the fundamental step in the analysis presented in Section 2.2. Eq. (6) can be written into a brief form as:

$$As^4 + Bs^3 + Cs^2 + Ds + E = 0, \tag{A1}$$

where

$$A = a_{11}, \quad B = -2a_{16}, \quad C = 2a_{12} + a_{66}, \quad D = -2a_{26}, \quad E = a_{22} \tag{A2}$$

To obtain the solution of Eq. (A1) we follow the method described by Neumark (1965). Eq. (A1) can be factorized into:

$$(As^2 + Gs + H)(As^2 gs + h) = 0 \tag{A3}$$

The coefficients G, H, g and h need to be determined, considering the resolvent cubic equation corresponding to Eq. (A1):

$$ax^3 + bx^2 + cx + d = 0 \tag{A4}$$

where

$$a = 1, \quad b = -2C, \quad c = C^2 + BD - 4AE, \quad d = -(BCD - B^2E - AD^2) \tag{A5}$$

The coefficients of Eq. (A3) can be represented as:

$$G = \frac{B + \sqrt{B^2 - 4Ax'}}{2}, \quad H = \frac{C - x'}{2} + \frac{B(C - x') - 2AD}{2\sqrt{B^2 - 4Ax'}}, \quad g = \frac{B - \sqrt{B^2 - 4Ax'}}{2},$$
$$h = \frac{C - x'}{2} - \frac{B(C - x') - 2AD}{2\sqrt{B^2 - 4Ax'}} \tag{A6}$$

where x' is a root of Eq. (A4), the expression of which follows:

$$x' = \frac{-b - 2\cos\left(\frac{\cos^{-1}\Delta}{3}\right)\sqrt{b^2 - 3ac}}{3a} \tag{A7}$$

where

$$\Delta = \frac{27a^2d + 2b^3 - 9abc}{2|b^2 - 3ac|^{3/2}} \tag{A8}$$

It should be noted that all the roots of the quartic equation will be complex when the cubic equation has three real roots. Its necessary condition is $0 \leq \Delta \leq 1$. The expression of x_1 in Eq. (A7) is valid under this condition.

Once the constants in Eq. (A6) are determined, one can easily find the roots of Eq. (A3) considering quadratic equations:

$$As^2 + Gs + H = 0 \quad \text{and} \quad As^2 + gs + h = 0 \tag{A9}$$

A.2. Derivation of equation for instantaneous rotation

Using the complex variable method in the plane theory of elasticity, Savin (1961) presented the instantaneous rotation (Ω) of an elliptical rigid inclusion hosted in infinite orthotropic matrix in terms of complex functions as:

$$\Omega = \frac{\mathrm{Re}[\mathrm{i}(Q_2(R - \mathrm{i}s_2)) - Q_1(R - \mathrm{i}s_1)]}{\mathrm{Re}[\mathrm{i}(P_1(R - \mathrm{i}s_1)) - P_2(R - \mathrm{i}s_2)]} \tag{A10}$$

where $R = a/b$, aspect ratio of inclusion and $s_1 = \alpha_1 + \mathrm{i}\beta_1$, $s_2 = \alpha_2 + \mathrm{i}\beta_2$. Re represents the real parts of the complex expressions in the numerator and denominator. P_1, P_2 and Q_1, Q_2 are complex functions. In order to find the instantaneous rotation Ω in Eq. (A10), the real and the imaginary parts of the expressions of these functions first need to be separated:

$$P_1 = \frac{Rp_2 + \mathrm{i}q_2}{2(p_1q_2 - p_2q_1)} \tag{A11}$$

In Eq. (A11) the parameters are complex. We have simplified them, and obtained their expressions as:

$$p_1 = I_1 + \mathrm{i}J_1, \tag{A12}$$

where $I_1 = (\alpha_1^2 - \beta_1^2)a_{11} + a_{12} - \alpha_1 a_{16}$ and $J_1 = 2\alpha_1\beta_1 a_{11} - \beta_1 a_{16}$

$$p_2 = I_2 + \mathrm{i}J_2, \tag{A13}$$

where $I_2 = (\alpha_2^2 - \beta_2^2)a_{11} + a_{12} - \alpha_2 a_{16}$ and $J_2 = 2\alpha_2\beta_2 a_{11} - \beta_2 a_{16}$

Similarly, the expressions of q_1 and q_2 follow:

$$q_1 = K_1 + \mathrm{i}L_1, \tag{A14}$$

where

$$K_1 = \alpha_1 a_{12} + \frac{\alpha_1}{\alpha_1^2 + \beta_1^2}a_{22} - a_{26} \text{ and } L_1 = \beta_1 a_{12} - \frac{\beta_1}{\alpha_1^2 + \beta_1^2}a_{22}$$

$$q_2 = K_2 + \mathrm{i}L_2, \tag{A15}$$

where

$$K_2 = \alpha_2 a_{12} + \frac{\alpha_2}{\alpha_2^2 + \beta_2^2}a_{22} - a_{26} \text{ and } L_2 = \beta_2 a_{12} - \frac{\beta_2}{\alpha_2^2 + \beta_2^2}a_{22}$$

Substituting the expressions in Eqs. (A12)–(A15) in the denominator of Eq. (A11), we have

$$p_1q_2 - p_2q_1 = M + \mathrm{i}N, \tag{A16}$$

where $M = I_1K_2 - J_1L_2 - I_2K_1 + J_2L_1$ and $N = I_1L_2 + J_1K_2 - I_2L_1 - J_2K_1$.

The real and the imaginary parts of the expression in Eq. (A11) then follow:

$$P_1 = A_1 + \mathrm{i}B_1, \tag{A17}$$

where

$$A_1 = \frac{M(RI_2 - L_2) + N(RJ_2 + K_2)}{2(M^2 + N^2)}, \quad B_1 = \frac{M(RJ_2 + K_2) - N(RI_2 - L_2)}{2(M^2 + N^2)}$$

Similarly, we have the expressions for P_2 as:

$$P_2 = \frac{Rp_1 + \mathrm{i}q_1}{2(p_1q_2 - p_2q_1)} = C_1 + \mathrm{i}D_1, \tag{A18}$$

where

$$C_1 = \frac{M(RI_1 - L_1) + N(RJ_1 + K_1)}{2(M^2 + N^2)}, \quad D_1 = \frac{M(RJ_1 + K_1) - N(RI_1 - L_1)}{2(M^2 + N^2)}$$

With the help of eq. 3.83 of Savin (1961), we have the expressions of Q_1 and Q_2 as follows:

$$Q_1 = \frac{1}{2(p_1q_2 - p_2q_1)}[B*'\{(R + \mathrm{i}s_1)(p_1q_2 - p_2q_1) + (R + \mathrm{i}\bar{s_1})(\bar{p_1}q_2 - p_2\bar{q_1})\} + (B*' - \mathrm{i}C*')(R + \mathrm{i}\bar{s_2})(\bar{p_2}q_2 - p_2\bar{q_2})] \tag{A19}$$

$$Q_2 = \frac{1}{2(p_1q_2 - p_2q_1)}[B^*(R + \mathrm{i}\bar{s_1})(\bar{p_1}q_1 - p_1\bar{q_1}) + (B*' + \mathrm{i}C*')(R + \mathrm{i}s_2)(p_2q_1 - p_1q_2) + (B*' - \mathrm{i}C*')(R + \mathrm{i}\bar{s_2}) \times (\bar{p_2}q_1 - p_1\bar{q_2})] \tag{A20}$$

where B^*, $B^{*\prime}$ and $C^{*\prime}$ are constants, which represent the far-field stresses. The expressions of these constants are:

$$B^* = \sigma^\infty \frac{\cos^2\alpha + (\alpha_2^2 + \beta_2^2)\sin^2\alpha + \alpha_2 \sin 2\alpha}{2[(\alpha_2 - \alpha_1)^2 + (\beta_2^2 - \beta_1^2)]} \tag{A21a}$$

$$B^{*\prime} = \sigma^\infty \frac{[(\alpha_1^2 - \beta_1^2) - 2\alpha_1\alpha_2]\sin^2\alpha - \cos^2\alpha - \alpha_2 \sin 2\alpha}{2[(\alpha_2 - \alpha_1)^2 + (\beta_2^2 - \beta_1^2)]} \tag{A21b}$$

$$C^{*\prime} = \sigma^\infty \left[\frac{(\alpha_1 - \alpha_2)\cos^2\alpha + [\alpha_2(\alpha_1^2 - \beta_1^2) - \alpha_1(\alpha_2^2 - \beta_2^2)]\sin^2\alpha}{2\beta_2[(\alpha_2 - \alpha_1)^2 + (\beta_2^2 - \beta_1^2)]} + \frac{[(\alpha_1^2 - \beta_1^2) - (\alpha_2^2 - \beta_2^2)]\sin\alpha\cos\alpha}{2\beta_2[(\alpha_2 - \alpha_1)^2 + (\beta_2^2 - \beta_1^2)]}\right] \tag{A21c}$$

With the help of Eqs. (A12)–(A16), Eq. (A19) can be expressed as:

$$Q_1 = E_1 + \mathrm{i}F_1, \tag{A22}$$

where

$$E_1 = \frac{M(x_1 + x_2) + N(y_1 + y_2)}{M^2 + N^2} \text{ and } F_1 = \frac{M(y_1 + y_2) - N(x_1 + x_2)}{M^2 + N^2}$$

$$x_1 = B^*[\{M(R - \beta_1) - N\alpha_1\} + \{(R + \beta_1)(I_1K_2 + J_1L_2 - I_2K_1 - J_2L_1) - \alpha_1(I_1L_2 - J_1K_2 + I_2L_1 - J_2K_1)\}]$$

$$y_1 = B^*[\{M\alpha_1 + N(R - \beta_1)\} + \{(R + \beta_1)(I_1L_2 - J_1K_2 + I_2L_1 - J_2K_1) + \alpha_1(I_1K_2 + J_1L_2 - I_2K_1 - J_2L_1)\}]$$

$$x_2 = 2(I_2L_2 - J_2K_2)[B^{*\prime}\alpha_2 - C^{*\prime}(R + \beta_2)]$$

$$y_2 = 2(I_2L_2 - J_2K_2)[B^{*\prime}(R + \beta_2) + C^{*\prime}\alpha_2]$$

Similarly, Eq. (A20) can be written as:

$$Q_2 = G_1 + \mathrm{i}H_1, \tag{A23}$$

where

$$G_1 = \frac{[M(u_1 + u_2 + u_3) + N(v_1 + v_2 + v_3)]}{2(M^2 + N^2)} \text{ and } H_1 = \frac{[M(v_1 + v_2 + v_3) - N(u_1 + u_2 + u_3)]}{2(M^2 + N^2)}$$

$$u_1 = -2\alpha_1(L_1I_1 - K_1J_1)B^*$$

$$v_1 = 2(R + \beta_1)(L_1I_1 - K_1J_1)B^*$$

$$u_2 = [B^{*\prime}\{(R-\beta_2)(I_2K_1 - J_2L_1 - I_1K_2 + J_1L_2) - \alpha_2(J_2K_1 + I_2L_1 - J_1K_2 - I_1L_2)\} - C^{*\prime}\{(R-\beta_2)(J_2K_1 + I_2L_1 - J_1K_2 - I_1L_2) + \alpha_2(I_2K_1 - J_2L_1 - I_1K_2 + J_1L_2)\}]$$

$$v_2 = [B^{*\prime}\{(R-\beta_2)(J_2K_1 + I_2L_1 - J_1K_2 - I_1L_2) + \alpha_2(I_2K_1 - J_2L_1 - I_1K_2 + J_1L_2)\} + C^{*\prime}\{(R-\beta_2)(I_2K_1 - J_2L_1 - I_1K_2 + J_1L_2) - \alpha_2(J_2K_1 + I_2L_1 - J_1K_2 - I_1L_2)\}]$$

$$u_3 = [B^{*\prime}\{(R+\beta_2)(I_2K_1 + J_2L_1 - I_1K_2 + J_1L_2) - \alpha_2(I_2L_1 - J_2K_1 - J_1K_2 + I_1L_2)\} + C^{*\prime}\{(R+\beta_2)(I_2L_1 - J_2K_1 - J_1K_2 + I_1L_2) + \alpha_2(I_2K_1 + J_2L_1 - I_1K_2 - J_1L_2)\}]$$

$$v_3 = [B^{*\prime}\{(R+\beta_2)(I_2L_1 - J_2K_1 - J_1K_2 + I_1L_2) + \alpha_2(I_2K_1 + J_2L_1 - I_1K_2 - J_1L_2)\} + C^{*\prime}\{(R+\beta_2)(I_2K_1 + J_2L_1 - I_1K_2 - J_1L_2) + \alpha_2(I_2L_1 - J_2K_1 - J_1K_2 + I_1L_2)\}]$$

Substituting the expressions of P_1 (A17), P_2 (A18), Q_1 (A22) and Q_2 (A23) in Eq. (A10), and then considering the real parts of the numerator and denominator of Eq. (A10), we have the instantaneous rotation:

$$\Omega = \frac{[F_1(R+\beta_1) - \alpha_1E_1] - [H_1(R+\beta_2) - \alpha_2G_1]}{[D_1(R+\beta_2) - \alpha_2C_1] - [B_1(R+\beta_1) - \alpha_1A_1]} \tag{A24}$$

References

Bjørnerud, M., 1989. Mathematical model for folding of layering near rigid objects in shear deformation. Journal of Structural Geology 11, 245–254.

Bjørnerud, M., Zhang, H., 1995. Flow mixing, object-matrix coherence, mantle growth and the development of porphyroclast tails. Journal of Structural Geology 17, 1347–1350.

Chandrupatla, T.R., Belegundu, A.D., 2001. Introduction to Finite Elements in Engineering, 2nd ed Prentice Hall, India p. 461.

Cobbold, P.R., 1976. Mechanical effects of anisotropy during large finite deformations. Bulletin of Geological Society of France 18, 1497–1510.

Fletcher, R.C., 2004. Anisotropic viscosity of a dispersion of aligned elliptical cylindrical clasts in viscous matrix. Journal of Structural Geology 26, 1977–1987.

Freeman, B., 1985. The motion of rigid ellipsoidal particles in slow flows. Tectonophysics 113, 163–183.

Gay, N.C., 1968. The motion of rigid particles embedded in viscous fluid during pure shear deformation of the fluid. Tectonophysics 5, 81–88.

Ghosh, S.K., Ramberg, H., 1976. Reorientation of inclusions by combination of pure shear and simple shear. Tectonophysics 34, 1–70.

Honda, S., 1986. Strong anisotropic flow in a finely layered asthenosphere. Geophysical Research Letters 13, 1454–1457.

Jeffery, G.B., 1922. The motion of ellipsoidal particles immersed in a viscous fluid. Proceedings of the Royal Society, London A 120, 161–179.

Jezek, J., Schulmann, K., Segeth, K., 1996. Fabric evolution of rigid inclusions during mixed coaxial and simple shear flows. Tectonophysics 257, 203–221.

Jezek, J., Stanislav, S., Segeth, K., Schulmann, K., 1999. Three-dimensional hydrodynamical modelling of viscous flow around a rotating ellipsoidal inclusion. Computers and Geosciences 25, 547–558.

Lekhnitskii, S.G., 1981. Theory of Elasticity of an Anisotropic Body. Mir Publishers, Moscow. 430pp.

Mandal, N., Chakraborty, C., Samanta, S.K., 2000. An analysis of anisotropy of rocks containing shape fabrics of rigid inclusions. Journal of Structural Geology 22, 831–839.

Mandal, N., Samanta, S.K., Chakraborty, C., 2001. Numerical modeling of heterogeneous flow fields around rigid objects with special reference to particle paths, strain shadows and foliation drag. Tectonophysics 330, 177–194.

Masuda, T., Ando, S., 1988. Viscous flow around a rigid spheroidal body: numerical simulation. Tectonophysics 148, 337–346.

Muskhelishvili, N.I., 1953. Some basic problems of the mathematical theory of elasticity. P. Noordhoff, Groningen. 695pp.

Neumark, S., 1965. Solution of Cubic and Quartic Equations. Pergamon Press, Oxford. 57pp.

Passchier, C.W., 1987. Stable positions of rigid objects in non-coaxial flow—a study in vorticity analysis. Journal of Structural Geology 9, 679–690.

Ramsay, J.G., Lisle, R., 2000. The Techniques of Modern Structural Geology, Applications of Continuum Mechanics in Structural Geology, vol. 3. Academic Press, London pp. 701–1061.

Savin, G.N., 1961. Stress Concentration around Holes. Pergamon Press, New York. 430pp.

Treagus, S.H., 2003. Viscous anisotropy of two-phase composites, and applications to rocks and structures. Tectonophysics 372, 121–133.

Weijermars, R., 1992. Progressive deformation in anisotropic rocks. Journal of Structural Geology 14, 723–742.